

Navigating seismic processing challenges for marine vibrator data

G. Poole¹, G. Jones¹, K. Cichy¹

¹ CGG

Summary

Marine vibrator sources offer the ability to emit a fully customisable and accurately repeatable sweep signature. Resulting peak amplitude levels are much lower than for airguns, making marine vibrators potentially preferable for the welfare of marine life. While the highly repeatable nature of the signal may be attractive for time-lapse applications, it must be considered alongside other time-lapse repeatability factors such as source positioning. The time-space variant nature of the marine vibrator emission creates self-blended recordings with source motion and Doppler shift effects, which must be corrected in processing. For frequency sweeps, a frequency-dependent spatial shift may be used alongside the traditional sweep correlation to correct the data to equivalent, stationary, zero-phase data. Synthetic tests using an inversion-driven alternative are shown to be robust and flexible for both frequency and band-limited pseudo-random sweeps. We show data examples from a marine vibrator field trial acquired in 2017. Although overall signal levels are consistent with airgun data, the final marine vibrator data shows some defocussing due to the data being acquired in several passes. We compare repeatability difference displays with and without the frequency-shift correction, confirming the expected benefit when applied.

Navigating seismic processing challenges for marine vibrator data

Introduction

Marine vibrator sources have been discussed in the literature for the past few decades (since Baeten et al., 1988) as a potential alternative to airguns. While airguns produce all their energy within a few milliseconds, marine vibrators typically take several seconds to emit the same energy levels. This results in significantly reduced peak sound exposure, which may be preferred for marine life (Hovem et al., 2012). While standard airguns indiscriminately emit energy over a wide frequency range, the output from marine vibrators may be focussed to a specified bandwidth for imaging or full-wavefield inversion. The emission of frequencies below the standard airgun range is possible by using very long monochromatic shakes, increasing the tow depth of marine vibrators, and using larger units with a low resonance frequency (Dellinger et al., 2016). Recently, large pneumatic airgun sources have become available as an alternative way to provide low-frequency signal (Shang et al., 2023). For simultaneous shooting applications, marine vibrator sources emitting different pseudo-orthogonal codes may help with deblending. The highly repeatable nature of the marine vibrator emission potentially makes it an ideal choice for time-lapse seismic projects.

While airgun sources emit all their energy from a fixed position in space, moving marine vibrators may travel several metres before they have emitted the same amount of energy. The marine vibrator source emission mixes in the subsurface, leading to a continual overlap of data being recorded, which must be corrected in data processing. While marine vibrator source emission repeatability provides a potential benefit for time-lapse projects, this must be considered alongside factors that cannot be controlled, such as the source position, as well as environmental changes such as water-column velocity, wave height, and tides. Another practical challenge is to ensure that there is enough space on the vessel to house the units required to produce a large enough source array. Other important factors to consider are the reliability of the units and ensuring that there is sufficient power available to drive them.

In this paper, we discuss some options for marine vibrator signature and motion correction and illustrate some observations using a real marine vibrator acquisition from the Norwegian North Sea.

Designature and source motion correction

As marine vibrators emit sweeps of several seconds in duration, the type of sweep signal used is critical to enable accurate decoding of the overlapping recorded signals. Frequency sweep signals offer an attractive option as the mutually orthogonal properties of different frequencies during the sweep allow for easy separation. The same slip-sweep approach used routinely with land vibroseis may also be adopted for marine vibrator frequency sweep applications. Pseudo-orthogonal signals offer an alternative; although not fully mutually orthogonal, they allow the potential for different sources to be encoded to help with deblending.

As well as sweep orthogonality, an understanding of source motion is critical to accurately process the data. Figure 1a shows a notional source following actuation of a 290 cu in airgun, derived using nearfield hydrophone measurements (Ziolkowski et al., 1982). The corresponding frequency-space (fx) display illustrates that all the energy is emitted at one location in space, and the resulting broadband spectrum contains significant bubble-pulse variations. Note that in the field, this notional source would be modified by the free-surface source ghost. Figure 1b shows the emission from a marine vibrator frequency sweep between 5 Hz and 25 Hz over a duration of 10 seconds. Based on a vessel speed of $2.5 \text{ m}\cdot\text{s}^{-1}$, the source will travel 25 m during the sweep. As shown on the fx display, this results in a frequency-dependent positional variation. Based on this observation, we propose to apply a source-motion correction by transforming the data to the frequency domain, applying a frequency-dependent spatial shift, and then reverse transforming back to the time domain. The result is shown in Figure 1c, where we have simulated data corresponding to a stationary marine vibrator, and all frequencies in the fx display are spatially consistent. At this point, we may correlate by the sweep, which results in the zero-phase wavelet shown in Figure 1d. After these corrections, the data may be processed as normal.

Figure 1e considers a 5 Hz to 25 Hz band-limited pseudo-random sweep. In this case, we emit all frequencies at all times during the sweep, and the method described for the frequency sweep will not work. The following section discusses an inversion-driven approach to handle this data.

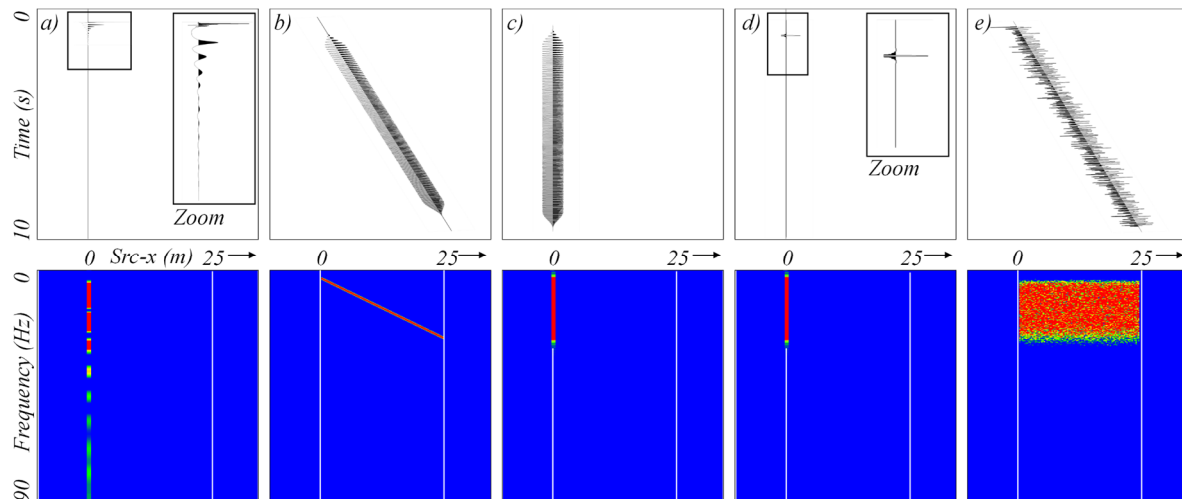


Figure 1 Comparison of airgun and marine vibrator signatures: a) Airgun, b) Marine vibrator frequency sweep, c) Frequency sweep after source motion correction, d) Frequency sweep after source motion correction and zero-phasing, and e) Marine vibrator pseudo-random sweep. Upper figures: signature in time and space; lower figures: frequency-space (f_x) representation.

To jointly compensate for the time-space nature of the marine vibrator emission, following Poole and Dowle (2019), we propose an inversion-based method built on a linear operator. The linear operator described by Equation 1 transforms a frequency-slowness ($f, j\Delta p$) model of standard receiver-domain data, m , to synthesise marine vibrator continuous recording data, r , at a stationary 0 receiver. In this notation, j is the slowness index and Δp is the slowness increment in $s \cdot m^{-1}$. The right-hand summation reverse slant-stacks the model to produce a trace relating to the marine vibrator source-receiver offset at each emission time, $k\Delta t$ (where k is the emission sample index and Δt is the emission sample rate in seconds). The reverse slant-stack time shift relates to the product of the model slowness in $s \cdot m^{-1}$ ($j\Delta p$) with the instantaneous offset ($vk\Delta t$; boat velocity, v , in $m \cdot s^{-1}$ multiplied by the emission time). The left-hand summation encodes the resulting reverse slant-stack trace with the discretised source emission value at that continuous recording time, $s(k\Delta t)$, and shifts it using the complex exponential.

$$r(f) = \sum_{k=0}^{k_{max}} s(k\Delta t) e^{-2\pi i f \cdot k\Delta t} \sum_{j=j_{min}}^{j_{max}} e^{-2\pi i f \cdot j\Delta p \cdot vk\Delta t} m(f, j\Delta p) \quad \text{Equation 1}$$

This linear system in the unknown m , may be solved in a least-squares sense. A standard reverse frequency-slowness transform may then output receiver gather data in the space-time domain with regular sampling for further processing. For efficiency, we may modify the expression to bin the source into time segments; this avoids a reverse f-p transform on to a fine offset interval. This inversion approach may be used for frequency or pseudo-random sweeps. We may optionally include the source ghost, solve in the time-domain, extend the formulation to 3D, or add sparseness constraints.

Figure 2a shows reference impulsive source synthetic data based on a constant velocity of $1500 m \cdot s^{-1}$ for a reflector at 400 m depth, producing a primary reflection followed by several orders of free-surface multiple. Source and receiver ghosts were not considered for this analysis. Figure 2b shows a simulation of marine vibrator continuous records using a frequency sweep from 5 Hz to 25 Hz emitted from a vessel moving at $2.5 m \cdot s^{-1}$. This was generated based on the modelling approach described in Equation 1. We see a continual overlap of energy in this simulation, including high-frequency wraparound energy at the top of the records. Figure 2c shows the result where we input the data of Figure 2b into the designation-source-motion inversion approach described above. This is an ‘inverse crime test’, where the same linear operator that produced the encoded data was used in the inversion problem. The result of this process (Figure 2c) accurately matches the reference data (Figure 2a), showing that the problem is invertible. In Figure 2d, we can see data simulated using a 5 Hz to 25 Hz band-limited random sweep. This sweep emits all frequencies at all times during the sweep. The random sweep decoding result is shown in Figure 2e, which overall looks similar to the frequency sweep result with the exception of additional random noise, particularly on the short offsets, due to the non-orthogonality of the sweep.

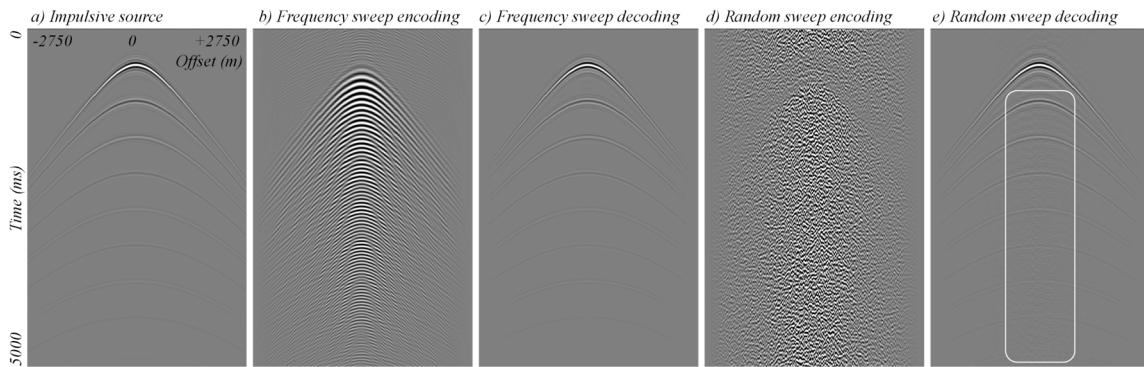


Figure 2 Blend-deblend tests: a) Impulsive source reference, b) Frequency sweep encoded data, c) Frequency sweep decoded data, d) Random sweep encoded data, and e) Random sweep decoded data.

Real data examples

The data examples come from 2D airgun and marine vibrator field tests acquired in the Norwegian North Sea in 2017 using low frequency (LF) and high frequency (HF) units recorded by ocean bottom nodes (OBN) (Teyssandier and Sallas, 2019). The shot-line was acquired several times using different frequency sweeps to build up a total frequency range from 3 Hz to 75 Hz as illustrated in Table 1. The source depth was varied to benefit from constructive source ghost interference.

<i>Marine vibrator unit type</i>	<i>Frequency range</i>	<i>Sweep length</i>	<i>Source depth</i>
<i>LF</i>	<i>3 to 6 Hz</i>	<i>40 seconds</i>	<i>24 m</i>
<i>LF</i>	<i>5 to 25 Hz</i>	<i>12 seconds</i>	<i>24 m</i>
<i>HF</i>	<i>20 to 40 Hz</i>	<i>20 seconds</i>	<i>11 m</i>
<i>HF</i>	<i>40 to 75 Hz</i>	<i>8 seconds</i>	<i>7 m</i>

Table 1 Marine vibrator frequency sweep acquisition information.

OBN receiver gather data from the four marine vibrator lines after source ghost, signature, and motion correction (based on the frequency-shift approach) are compared with consistently bandpass-filtered airgun data after source deghosting and designature in Figure 3. Generally, there is a good phase match between the airgun and marine vibrator data, which confirms the source correction approaches for both data types. Towed at 7 m depth, the 290 cu in airgun volume was chosen to have a similar overall amplitude level, which can be qualitatively confirmed by these displays. The 3-6 Hz marine vibrator display (Figure 3a) has higher signal levels compared to the airgun data, due to the increased source depth, provided by constructive interference at the source ghost peak.

These marine vibrator and airgun data were processed through a sequence including source deghosting, demultiple, and migration. Figure 4a shows the airgun result, and Figure 4b shows the composite result from the marine vibrator acquisitions. While the signal-to-noise ratio is similar for both images, the marine vibrator result is less well focussed due to different frequency ranges being acquired with slightly different source locations in this 2D test. Marine vibrator data was reacquired in the opposite shooting direction. Focussing on a window of data (Figure 4c), Figures 4d and 4e show marine-vibrator-on-marine-vibrator 4D differences before and after source motion correction, respectively. As expected, 4D differences are reduced with the use of source motion correction, especially on the steeper dips.

Conclusions

We have discussed how to correct the time-space nature of moving marine vibrator data. A frequency-shift method is suited to frequency sweep acquisition, while an inversion-based method is available for other emissions, such as pseudo-random sequences. We have compared data from airgun and marine vibrator acquisitions in the Norwegian North Sea. The overall signal content was similar, but the marine vibrator result was not as well focussed due to different frequencies being acquired independently. Marine vibrator 4D difference sections improved with the use of source motion correction.

Acknowledgements

We thank CGG and Sercel for the permission to publish this paper and share the real data examples. Thanks to Simon King for his help in preparing some figures.

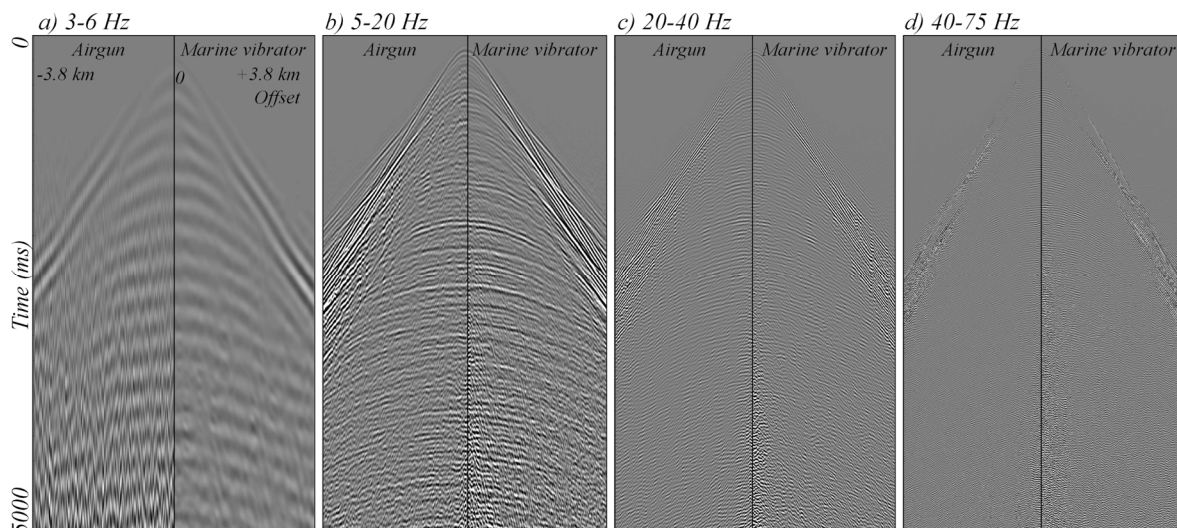


Figure 3 Comparison of airgun and marine vibrator data in different frequency bands as annotated.

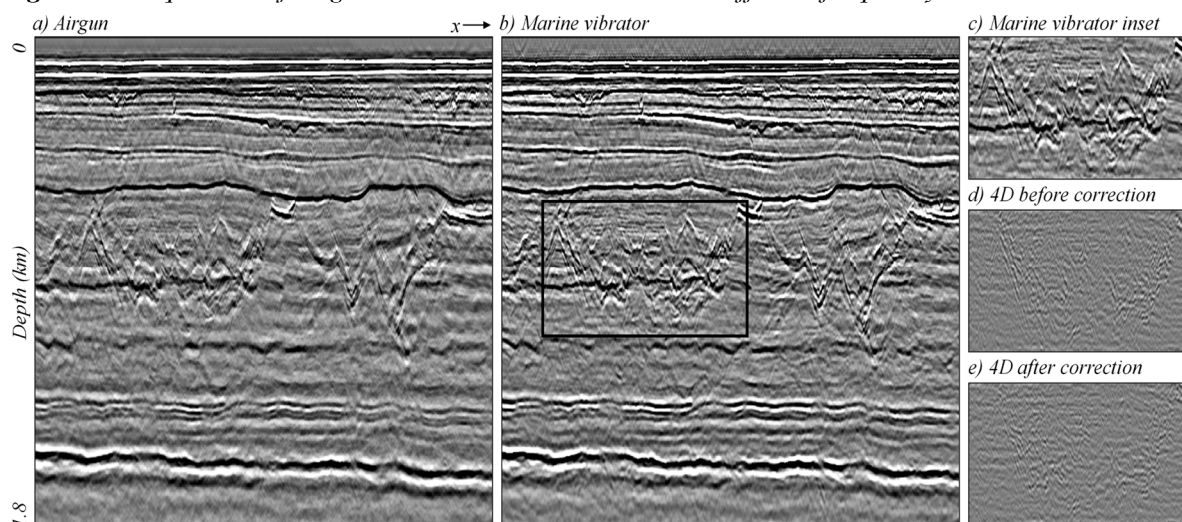


Figure 4 Migrated data comparison: a) Airgun, b) Marine vibrator, c) Marine vibrator inset display, and Marine vibrator difference d) before, and e) after source motion correction.

References

- Baeton, G., Fokkema, J. and Ziolkowski, A. [1988] The marine vibrator source. *First Break*, **6**(9), 285-294.
- Dellinger, J., Ross, A., Meaux, D., Brenders, A., Gesoff, G., Etgen, J.T., Naranjo, J., Openshaw, G. and Harper, M. [2016] Wolfspar®, an “FWI-friendly” ultra-low-frequency marine seismic source. *86th SEG Annual International Meeting*, Expanded Abstracts, 4891–4895.
- Hovem, J. M., Tronstad, T.V., Karlsen, H.E. and Lokkeborg, S. [2012] Modeling propagation of seismic airgun sounds and the effects on fish behavior. *IEEE Journal of Oceanic Engineering*, **37**(4), 576–588.
- Poole, G. and Dowle, R. [2019] Method for designature of seismic data acquired using moving source. *Granted US Patent 10,288,753*.
- Shang, X., Kryvohuz, M., Macintyre, H., Baeten, G., Allemand, T., Herrmann, P., Laroche, S. and Ronen, S. [2023] Broadband data with a new low frequency source — Acquisition and processing example from the Gulf-of-Mexico. *Third International Meeting for Applied Geoscience & Energy*, Expanded Abstracts, 142-146.
- Teyssandier, B. and Sallas, J. [2019] The shape of things to come – Development and testing of a new marine vibrator source. *The Leading Edge*, **38**(9), 680-690.
- Ziolkowski, A., Parkes, G.E., Hatton, L. and Haugland, T. [1982] The signature of an airgun array: computation from near-field measurements including interactions. *Geophysics*, **47**(10), 1413-1421.